www.czasopisma.pan.pl PAN www.journals.pan.pl
POLSKA AKADEMIA NAUK

ARCHIVES
of
FOUNDRY ENGINEERING

DOI: 10.1515/afe-2017-0040

Published quarterly as the organ of the Foundry Commission of the Polish Academy of Sciences

DE GRUYTER OPEN

ISSN (2299-2944)
Volume 17
Issue 1/2017

228 – 234

Application of FEM Analysis for Evaluation of the Stress and Deformation Distributions in the Top Layer of A390.0 Alloy During Friction

R. Wieszała *, [a], J. Piątkowski [b], H. Bąkowski [a]
Silesian University of Technology, [a] Faculty of Transport, [b] Faculty of Materials Engineering and Metallurgy
Krasińskiego 8, 40-019 Katowice, Poland
*Corresponding author. E-mail address: robert.wieszala@polsl.pl

Received 05.04.2016; accepted in revised form 07.02.2017

Abstract

The paper presents an analysis of the effect of shape of primary silicon crystals on the sizes of stresses and deformations in a surface layer of A390.0 alloy by Finite Elements Method (FEM). Analysis of stereological characteristics of the studied alloy, performed based on a quantitative metallographic analysis in combination with a statistical analysis, was used for this purpose. The presented simulation tests showed not only the deposition depth of maximum stresses and strains, but also allowed for determining the aforementioned values depending on the shape of the silicon crystals. The studied material is intended for pistons of internal combustion engines, therefore the analysis of the surface layer corresponded to conditions during friction in a piston-cylinder system of an internal combustion engine having power of up to 100 kW. The obtained results showed important differences in the values of stresses and strains up to 15% between various shape of the silicon crystals. Crystals with sharp edges caused higher stresses and deformation locally than those with rounded shapes.

Keywords: Hypereutectic Al-Si alloy, Surface layer, Finite Elements Method (FEM)

1. Introduction

Properties of Al-Si cast alloys are determined by the condition of their structure, mainly by size of intermetallic phases and their distribution in the matrix, as well as by eutectic morphologies. As the silicon content approaches hypereutectic composition, the influence of the refinement of grains containing solid solution dendrite families decreases, and the significance of the morphology of primary silicon crystals and their uniform distribution in the matrix increases. The most frequently occurring forms of primary silicon in hypereutectic silumins are as follows: star-shaped form, polyhedral form, dendritic form (in case of rapid cooling), and ornament form [1, 2]. They are precipitations assuming structures of, among others, radial plates, needles, polyhedrons, long-pointed stars – unfavourable from the point of view of performance and machinability of hypereutectic silumins [3-5]. Such an unfavourable structure may be, among others, transformed in the result of a modification with, for instance, individual or combined phosphorus-based, titanium-based and boron-based master alloys [6, 7]. The modification carried out is intended for an increase in density of heterogeneous washers, hinder nucleation of silicon crystals, thus limiting their growth. However, it should be noted that the silicon crystals refinement itself is sometimes not sufficient. It is also necessary to obtain proper shapes of silicon crystals approaching spheroidisation. As an example, modified fine-grained silicon crystals with sharp edges having an adverse effect on e.g. tribological properties, may be named. The heat treatment carried out allows for reducing this effect by rounding the edges, however the shape of primary silicon crystals remains unchanged [8]. Moreover, the distribution of the individual eutectics and the primary silicon crystals has a significant influence on the fatigue strength of silumins, e.g. by exposition of microcracks after the silicon crystal boundary [9].

Constantly increasing technical requirements, connected with the development of construction of internal combustions engines, require also changes in the material properties. Development of completely new materials is very costly [10], therefore works on improvements of already existing materials are carried out. To this end, it is necessary to develop manufacturing processes enabling a multidirectional optimisation, taking current needs into account. Determination of the direction of changes and needed operational properties of materials are often obtained from computer simulations, which allow, at their current technical level, for relatively accurate representation of actual operating conditions, and pertain to many aspects without a necessity for costly real tests [11]. Simulation tests of car pistons allow, among others, for defining the temperature distribution in the individual phases of the piston operation, and with given variable parameters [12].

Usability evaluation of a material depends on many factors. These include proper stress and deformation distributions in the top layer [13, 14]. For this purpose, computer simulations are applied, which allow for determining the distributions of the individual values, however it requires creation of a proper computer model [15]. An additional difficulty is posed by the fact that, due to changes in the structure, often slight and nevertheless important, the models being created are suitable only for the given material, and thus, development of separate models for every material is necessary [16].

In the paper, simulation tests using FEM technique are presented, which allow for defining the influence of the shape of primary silicon crystals on the distributions of stresses and deformations, and on the size of the top layer during friction, by modeling the operating conditions of an internal combustion engine piston in an association with a typical material used for cylinder barrels – GJL-350 cast iron.

2. Aim and scope of the studies

The aim of the paper is to evaluate the effect of size and shape of primary silicon crystals on the stress and deformation distributions in the top layer of A390.0 alloy during friction. To this end, the scope of the work includes, among others, creation of an FEM model, representing the stress and deformation distributions in the studied alloy during friction in an association with GJL-350 cast iron.

3. Material and methodology

An A390.0 alloy, used for heavy duty casts of pistons and heads of internal combustion engines, engine blocks and cylinder bodies, was selected for the research. The studied silumin was melted in a Balzers VSG induction furnace using pure aluminium (purity 99.96%), silicon, AlCu50 master alloy (PN-EN 575), and AG10 alloy (10% by wt. Mg) in an SiC crucible. For the modification, a CuP10 master alloy (0.05% by wt. of the alloy) and Protecol-Degasal mixture (0.4% by wt.) were used, and 0.2% by wt. of Rafglin-3 preparation was introduced below the layer of the formed slag. After approx. 10 minutes, the formed slag was removed and the alloy was cast to a standard ATD sampler (Heraeus Elektro-Nite), obtaining samples for further tests. Results of analysis of chemical composition of the A390.0 alloy are presented in Table 1. GJL-350 cast iron with flake graphite in a pearlitic matrix was used as a counter sample. A model of the association is shown in Fig. 1. All dimensions in micrometers.

Table 1.
Chemical composition of the A390.0 silumin (% by wt.)

	Si	Cu	Mg	Mn	Fe	Ni	Al
alloy	16.81	4.78	0.94	0.03	0.04	0.13	remainder

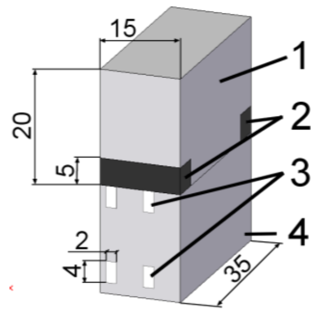

Fig. 1. An exemplary model of the analysed association, with dimensions: 1) GJL-350 cast iron, 2) graphite, 3) silicon crystals, 4) A390.0

Pressure of the piston onto the cylinder barrel amounted to 3 MPa in the tested model, with a friction coefficient of 0.3 [17]. The solid model of a cast iron-composite sliding contact with applied forces is presented in Fig. 2.

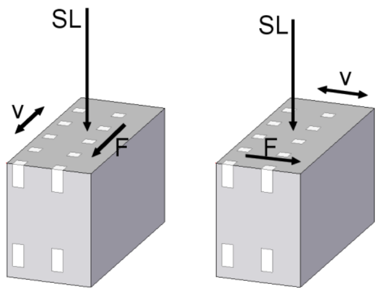

Fig. 2. A390.0 solid model with selected boundary conditions: SL – surface load, F – friction force, v – motion direction

In order to determine stereological characteristics, quantitative metallographic analysis was used, which, while combined with statistical analysis, enables determination of statistical distributions and quantities necessary for an objective evaluation of the structure. The quantitative metallographic analysis is used for numerical determination of number of objects, their dimensions, shapes and distributions (stereological characteristics). It yields a set of numbers describing the characteristics of a structure. Strict dependencies (correlations) between the structure and the properties, as well as between the structure and the parameters of a manufacturing or operating process, may be found only in quantitative metallography defined by the number and unit of measure.

Measurement of the stereological characteristics of wear products is possible thanks to a digital image analysis system. Statistical analysis of the obtained measurement data includes classification to corresponding size classes and calculation of basic statistical quantities. The quantitative analysis yields a set of numbers and graphs describing the selected characteristics of the studied object. In Fig. 3, an exemplary shape of a primary silicon crystal is shown. Results of statistical analysis of primary silicon crystals are gathered in Table 2, while Fig. 4 shows the shape of primary silicon crystals adopted for the FEM analysis.

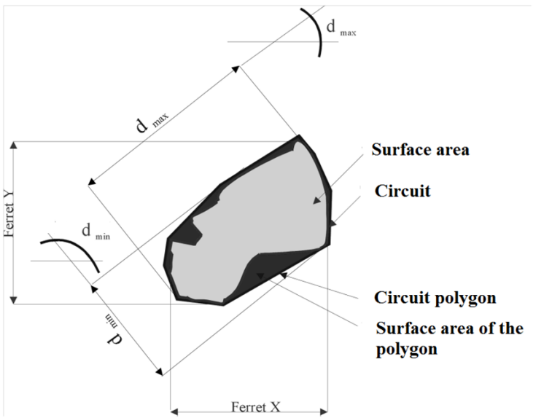

Fig. 3. Stereological features of the studied objects

Table 2.
Stereological parameters of primary silicon crystals in the A390.0 alloy.

Stereological parameters	SM	SP	SPM
Surface area, μm^2	13.0	13.0	12.0
Circumference, μm	7.0	7.0	9.0
Shape coefficient	0.7	0.7	0.5
Diameter, μm	2.8	2.9	3.0
Max diameter, μm	3.4	3.7	3.7
Min diameter, μm	1.8	1.9	2.0
Intermolecular distance, μm	4.8	4.7	4.7

where: SM – modified alloy with CuP, SP – superheated alloy, SPM – modified with CuP and superheated alloy

Construction of a proper geometric model of a machine part being analysed is a quite complex task. The difficulty level depends on the degree of complexity of the part, on the assumed accuracy of representation of the given part in the model and on the user's abilities to use CAD software. The geometric model may be simplified, facilitating its creation and shrotening the calculation time.

The boundary conditions in the developed model were selected so at to represent conditions in the actual system of a piston-cylinder association in an internal combustion engine. The selection of the conditions determines the final results and distributions of the obtained stresses and dislocations. Using simulation analysis, it is possible to determine wear-initiating spots, i.e. the spots of occurrence of maximum stress and dislocation values, as well as change in stress senses.

4. Finite Elements Method

Currently, the Finite Elements Method (FEM) is one of basic methods of computer-aided engineering calculations (CAE). Also in construction and operation of internal combustion engines, the manufacturing process may be simplified or the damage causes of a selected component may be explained by construction of a proper model of the analysed object and calculations by the Finite Elements Method. Intending to map fully the real object and its real operating conditions, and interpret correctly the obtained calculation results of one must have knowledge not only on mechanics, but also physics and machinery & equipment operation, including tribology. In order to use the FEM, construction of proper models of the analysed machine parts is necessary (Fig. 4, Table 3). Table 3 presents the material constants of each phase in the structure necessary for the implementation numerical calculations.

Table 3.
Selected parameters necessary for construction of a model of the piston-cylinder barrel association [2]

Structural elements	Young modulus, MPa	Poisson number	Density, kg/m^3
A390.0	70000	0.36	2730
GJL-350	140000	0.26	7450
Graphite	4800	0.20	2250
Silicon	112000	0.28	2329

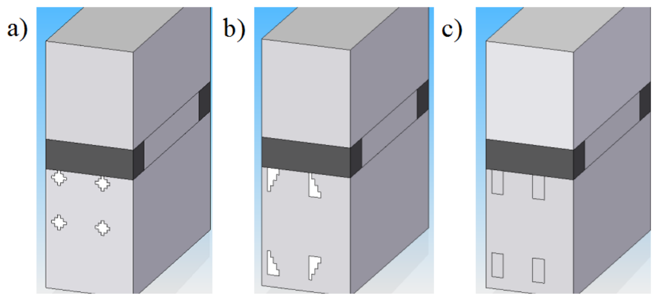

Fig. 4. Solid models of the piston-cylinder barrel association: a) round crystal, b) sharp crystal, c) reference crystal

To this end, the Authors performed the following operations:

- defining the construction geometry model,
- selection of the element type,
- creation of a grid of finite elements,
- defining the properties of materials,
- defining the properties of elements,
- verification of the quality of the finite element grid,
- introduction of loads and boundary conditions,
- specification of the type of the requested analysis,
- defining the requirements for the quantity and type of results,
- interpretation of the obtained results.

The structure siliminu used connection Bonded type. The nodes on the two edges are concerted and the analysis will be able to move freely independently of each other. The movement of nodes to each other will be held with the resistance that determines stiffness. contact stiffness is calculated automatically from the geometry and the material properties of the parts, the value is automatically adjusted based on the current status of the contact (eg., penetration or no penetration) This makes it increases the accuracy and convergence of the real object.
The second parameter is the tolerance of the contact or the contact distance between any nodes on the surface where contact occurs. besides important parameters are the distance of contact interaction and the maximum length of penetration or the maximum initial distance. All parameters Kontact are selected empirically. There is no single set of parameters that lead to accurate solution for all models. Many of the models analyzed contact is your solution without any problems using standard settings, while some require a certain interference. A proper understanding of engineering issues and functionality of each parameter has allowed them to select the appropriate set for a particular task. This requires a lot of experience and time. Between cooperating materials A390.0 / GJL-350 occurs friction contact according to Coulomb's law. Sliding kinetic friction value is 0.1. The pressure surface A.390.0 to GJL-350 was 3 MPa. The values have been chosen for the help of experimental research and analysis of the literature [25].

4.1. Validation rule

The most labor-intensive and time-consuming stage of FEA is to divide the area into finite elements. Selection of appropriate elements discretization area has a significant effect on obtaining correct results. Geometric model has been divided into a finite number of finite elements using a mesh type of Hexa. Hexa mesh is the most demanding in terms of effort and user program progress. This solution is mainly used for analysis, which because of its type disqualify the use of type tetra mesh and when it is important to the quality of the mesh [24, 26].

The correctness of the FEM grid was verified using Jacobian determinant, which should be lower than 0.6 (Fig. 5). In this way, the obtained results of σ/ε distributions will not be burdened with errors. The correctness of the results can be verified on the basis of formulas Hertz, however designated distributions of stresses and strains and their values using the MES allows the determination of local stress concentrations, often exceeding the maximum shear stresses. Much information on application of the FEM for verification of designed machine parts, including vehicle parts [18-23], may be found in the literature. However, finding information on application of the FEM for explanation of causes and mechanisms of machine parts wear is more difficult, as they are scattered in scarce literature dealing with issues of the FEM, engine construction and tribology [24]. Paper [24] is focused on reduction of a piston weight while taking into account the high mechanical and thermal loads experienced. Authors of [25] dealt with explanation of piston damage mechanisms using the FEM analysis. In the paper, changes in stresses and deformations in the top layer of the piston-cylinder barrel associationm during friction were analyzed.

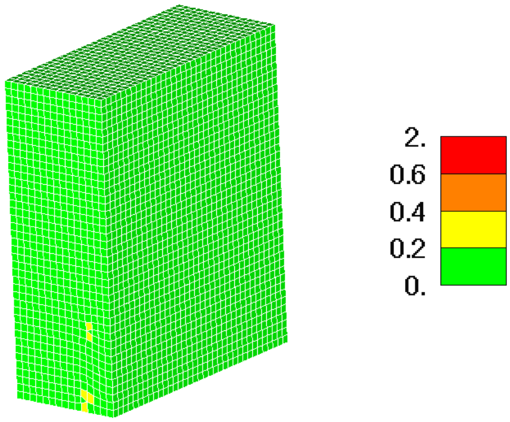

Fig. 5. Jacobian determinant

5. Results and their analysis

Friction forces affecting the analysed association were oriented along the graphite precipitations (direction I) and transversely to them (direction II). The presented cross-sections along the analysed model allowed for determining stresses and deformations in the area of graphite-silumin interaction (cross-section A) and in the area of pearlite-silumin interaction (cross-section B), shown in Fig. 6. In the result of the FEM analysis, distribution of stresses (σ) and deformations (ε), and their values were obtained (Figs. 7, 8, 9).

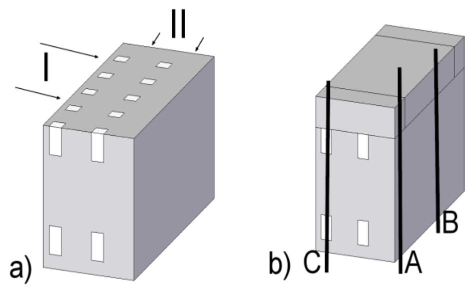

Fig. 6. Postprocessing: I – motion along the graphite fibres, II – motion transversely to the graphite fibres (a), and analysed model cross-sections modelu (b)

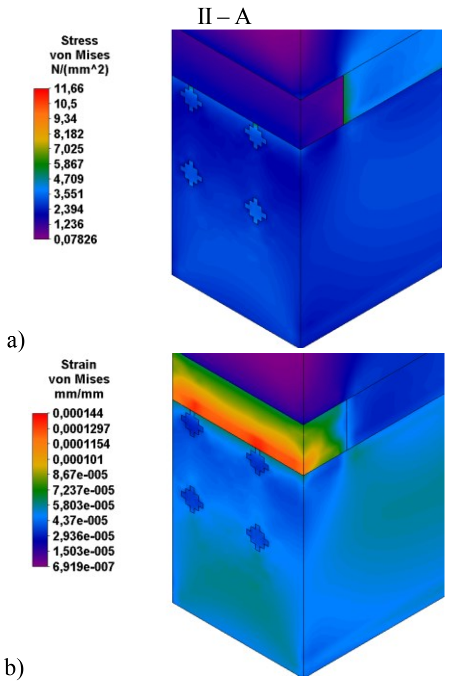

Fig. 7. Distribution of stresses (a) and deformations (b) during friction transverse to the graphite fibres in a graphite-silumin contact

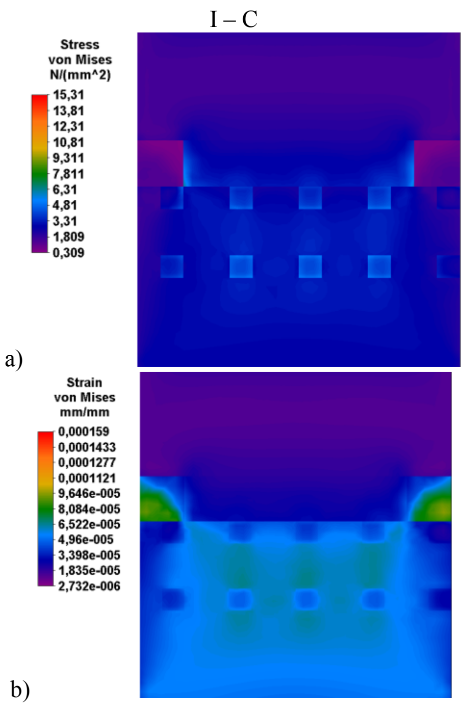

Fig. 8. Distribution of stresses (a) and deformations (b) during friction along the graphite fibers in a graphite-pearlite-silumin contact

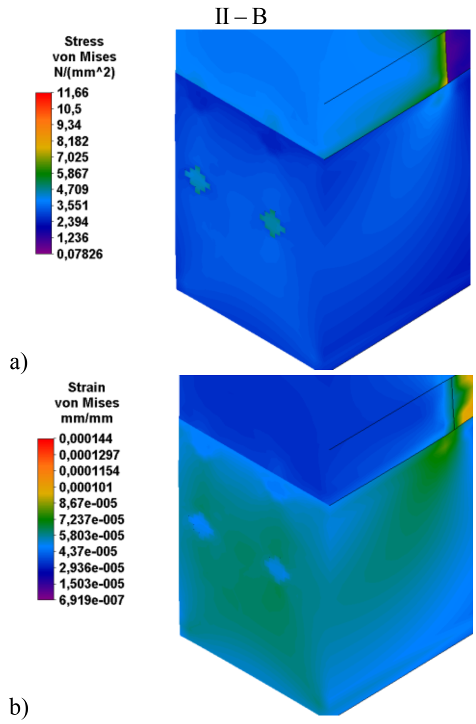

Fig. 9. Distribution of stresses (a) and deformations (b) during friction transverse to the graphite fibres in a pearlite-silumin contact

Figure 7 shows the distribution of of stresses and strains, so that it was found that due to the shear stress reaches the chipping the graphite of cast iron matrix. This is because of exceeding the the allowable stresses for the graphite (which are approx. 1-2 MPa), where the calculation model of MES stresses exceed the value of 2 MPa.

The shown results of distributions and values of stresses and deformations allowed for presenting important differences in gthe deposition depth of maximum stresses and deformations. In these locations decohesion and cracking of not only the matrix, but also the silicon grains (crystals) themselves (Fig. 10) may occur.

In the locations where the silumin contacts with the cast iron, the values of stresses and deformations, as well as the depth at which the aforementioned values affect, change and have a different distribution. It pertains to the silumin-pearlite contact (Fig. 9. a, b) or silumin-graphite contact (Fig. 7. a, b). Both in the matrix and in the silicon crystals in the silumin-pearlite contact, values of stresses are twice as high (ca. 6 MPa) as in the silumin-graphite contact (ca. 3 MPa). In Table 4, the results of simulation tests sing FEM, depending on the shape of the silicon crystals in the A390.0 silumin are collected. The highest stress σ values were obtained for the motion along the graphite fibres (I) and transversely to the graphite fibres (II), for the silumin/graphite contact with a sharp shape of the silicon crystal. They amounted to approximately 23.5 MPa. The lowest stress σ values were obtained for the silumin/pearlite contact, in transverse motion with respect to the fibres, for the sharp shape and the reference shape. They amounted to approximately 10.5 MPa.

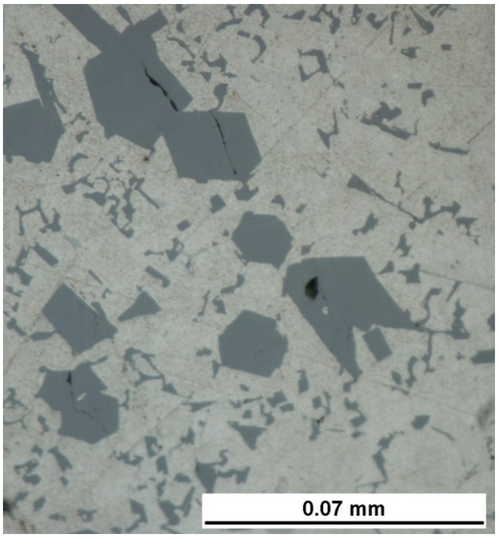

Fig. 10. Crystals cracked due to the fatigue

Table 4.
List of results of the simulation tests in the piston/cylinder barrel association

Shape of the silicon crystal	Motion direction – along the graphite fibres (I)	Motion direction – transversely to the graphite fibres (II)	
		Silumin/pearlite contact	Silumin/graphite contact
	σ/ε	σ/ε	σ/ε
	23.37 [MPa] — 0.0002471	10.42 [MPa] — 0.0001508	23.59 [MPa] — 0.0002677
	15.11 [MPa] — 0.0001590	11.66 [MPa] — 0.0001440	15.31 [MPa] — 0.0001370
	14.21 [MPa] — 0.0001357	10.95 [MPa] — 0.0001432	14.61 [MPa] — 0.0001558

An analogous situation occurs in the case of deformations ε, where the highest values have been obtained for the sharp shape of the silicon crystal and for transverse motion with respect to the graphite fibres (II) and along the graphite fibres. They amounted to approximately 0.0002677. The lowest deformation ε values have been obtained for the reference crystal in motion along the graphite fibres. They amounted to 0.001357.

The obtained results indicate unequivocally that a change in the shape of the silicon crystal translates into the values of stresses and deformations in the top layer. It is also noteworthy that a structure refinement and formation of fine-grained silicon crystals with sharp edges will affect adversely the tribologic properties of the studied alloy.
The presented results of simulation tests defined not only the deposition depth of maximum stresses and deformations (Figs. 7, 8, 9), but also allowed for determining the aforementioned values depending on the shape of the silicon crystals. The sharper shapes they have, the higher the analysed initial values in the FEM program are. The goal of the silumin modification is to obtain silicon crystals close to spheroidal shapes. It will allow for obtaining low values of stresses and deformations, which will not cause cracking both in the alloy matrix, and in the crystals, themselves.

5. Summary

Application of the FEM analysis allowed for determining a difference in values of stresses and deformations for the assumed shapes of primary silicon crystals. The analysis revealed significant differences between the individual shapes of silicon crystals, reaching 15%. Crystals with sharp edges caused higher stresses and deformation locally than those with rounded shapes. One should note that the performed analysis took into account local stresses occurring within the material during friction. It allows for presenting the distribution of stress values and the deposition depth of deformations which could cause local decohesions. However, no changes in the deposition depth of deformations were observed for the studied materials during detailed analyses.

The analysis carried out for the studied materials reveals that even slight changes in the materials structure translate into visible changes in material properties, including the simulated values of stresses and deformations in the top layer. For the sake of the material specificity, a comparison of the obtained results with those for other materials is not possible, because it is necessary to construct a separate FEM model for each structure. It should be mentioned that tests of such a type are rare and they are published seldom because of technological secrets. Therefore, new manufacturing technologies should be treated carefully. Before they are implemented in practical use, a thorough identification of changes, even those seemingly insignificant, is necessary.

References

[1] Piątkowski, J. (2009). The phosphorus interaction on the process forming of primary structure of hypereutectic silumins. *Archives of Foundry Engineering*. 9(3), 195-199.

[2] Piątkowski, J. (2013). *Physical and chemical phenomena affecting structure, mechanical properties and technological stability of hypereutectic Al-Si alloys after overheating*. Gliwice: Wyd. Politechniki Śląskiej.

[3] Min Zuo, Kun Jiang, Xiangfa Liu. (2010). Refinement of hypereutectic Al-Si alloy by new Al-Zr-P master alloy. *Journal of Alloys and Compounds*. 503, 126-130.

[4] Binczyk, F., Piątkowski, J. & Smoliński A. (2000). The mechanism of interaction of phosphorus in the process

of modifying Silumin hypereutectic. *Solidfication fo Metals and Alloys*. 43, 21-26.
[5] Romankiewicz, F. (2000). Modyfication of silumin AK20. *Solidification of Metals and Alloys*. 44, 318-322.
[6] Piątkowski, J. & Gajdzik, B. (2013). Testing phase changes in Al-Si cast alloys with application of thermal analysis and differential calorimetric analysis. *Metalurgija*. 52(4), 469-472.
[7] Piątkowski, J. (2009). Development of the fundamentals of melting and casting technology of Al-Me (Cr, Ni, Mo, W, Ti) master alloys used for modification of microstructure in silumins. *Archives of Foundry Engineering*. 9(2), 17-21.
[8] Sudha, J., Kumar, S. & Prasath, B. (2015). Compressive flow behavior of Al-Si based alloy: Role of heat treatment. *Material Science & Engineering A*, 629, 41-53.
[9] Mbuya, T.O. & Reed, P.A.S. (2014). Micromechanisms of short fatigue crack growth in an Al-Si piston alloy. *Material Science & Engineering A*. 612, 302-309.
[10] Oczoś, K., Kawalec, A. (2012). *Formation of light metals.* Warszawa: Wydawnictwo Naukowe PWN. (in Polish).
[11] Haniszewski, T. (2014). Strength analysis of overhead traveling carne with use of finite element method. *Transport Problems*. 9, 19-26.
[12] Buyukkaya, E. (2008). Thermal analysis of functionally graded coating AlSi alloy and steel pistons. *Surface & Coatings Technology*. 202, 3856-3865.
[13] Deguan Shi, Dayong Li, & Guili Gao. (2008). Relation between surface tension and microstructural modification in Al-Si alloys. *Materials Characterization*. 59, 1541-1545.
[14] Sathyapal, H. & Prabhu, K.N. (2008). Modification of eutectic silicon in Al-Si alloys. *Journal of Materials Science*. 43, 3009-3027.
[15] Zhen-qiang, W., Yuan, X., Guang, L. & Fang-tao, X. (2007). Finite element analysis on stresses field of normalized layer thickness within ceramic coating on aluminized steel. *Transcactions of Nonferrous Metals Society of China*. 17, 934-939.
[16] Sudha, J., Kumar, S., Bhadram, V. & Narayana, Ch. (2015). Stress states in individual Si particles of a cast Al-Si alloy: Micro-Raman analysis and microstructure based modeling. *Journal of Alloys and Compounds*. 625, 296-308.
[17] Wieszała, R. & Piątkowski, J. (2016). Analysis of surface coarseness for friction node of alloy AlSi17Cu5 and cast-iron EN-GJL-350. *Solid State Phenomena*. 246, 1662-9779.
[18] Dongchan, L., Yoonhwan, W., Sangho, L. & Changsoo, H. (2008). Design consideration of the nonlinear specifications in the automotive body. *Finite Elements in Analysis and Design*. 44, 851-861.
[19] Knez, M., Glodez, S. & Kramberger, J. (2009). Fatigue assessment of piston rod threaded end. *Engineering Failure Analysis*. 16, 1977-1982.
[20] Wanga, Z.W., Luo, Y.Y., Zhou, L.J., Xiao, R.F. & Peng, G.J. (2008). Computation of dynamic stresses in piston rods caused by unsteady hydraulic loads. *Engineering Failure Analysis*. 15, 28-37.
[21] Silva, F.S. (2006). Fatigue on engine pistons – A compendium of case studies. *Engineering Failure Analysis*. 13, 480-492.
[22] Gąska, D. & Pypno, C. (2011). Strength and elastic stability of cranes in aspect of new and old design standards. *Mechanika*. 17, 226-231.
[23] Patel, P. & Patel, V.K. (2013). A review on structural analysis of overhead crane girder using FEA technique. *International Journal fo Engineering Science and Innovative Technology*. 2, 41-44.
[24] Bąkowski, H. & Stanik, Z. (2010). Applications of FEM for explanation of influence of the operating parameters upon failure wear of the piston in a diesel engine. *Mechanik*. 4, 298-299.
[25] Posmyk, A. & Bąkowski, H. (2013). Wear mechanism of cast iron piston ring/aluminum matrix composite cylinder liner. *Tribol. Trans.* 56(5), 806-815.
[26] Nicholson, D.W. (2005). Stiff are length constraint in nonlinear FEA. *Acta Mechanica*. 175, 123-137.